Academic Science Journal

Preparation and Characterization of TiO_2 Nanoparticles via a Sol- gel Method

Maryam S. Jabbar[1], Olfat A. Mahmood*[1] and Zainab N. Jameel[2]

[1]Department of Physics, College of Science, University of Diyala

[2]Communication Engineering Department, University of Technology

*olfatahmed183@gmail.com

Received: 17 September 2023 **Accepted: 22 December 2023**

Published: January 2025

DOI: https://dx.doi.org/10.24237/ASJ.03.01.821C

Abstract

TiO_2 nanoparticles (NPs) were prepared by the sol-gel method by using $TiCl_4$ as a starting material, whereas the applied temperatures were 450 °C and 900 °C. The XRD results showed that nanoparticle (TiO_2 NPs) anatase and rutile phases had a polycrystalline nature with a tetragonal structure. FESEM results showed the formation of nanostructures with cauliflower and irregular shapes with average particle sizes of 36.9 nm and 58 nm for the Anatase and Rutile phases, respectively. The EDS spectra showed that the elements present in the synthesized TiO_2 NP (anatase and rutile) phases were Ti and oxygen O. The FTIR spectra of TiO_2 NPs showed the presence of broadband at 450–4000 cm^{-1} corresponding to the stretching vibration of terminating hydroxyl groups in the samples. The UV–Vis-NIR absorbance spectra were recorded in the range of 300–900 nm to investigate the optical characteristics. Results showed that the absorption of TiO_2 in the Anatase phase is less than that of TiO_2 in the Rutile phase. The optical energy gaps were 3.05 and 2.7 eV for the Anatase and Rutile phases, respectively.

Keywords: TiO_2, Anatase phase, Rutile phase, FE-SEM, EDS.

Introduction

The past few decades have witnessed a remarkable increase in people's interest in research in nanotechnology. Given that nanoparticles (NPs) have different physical and chemical properties compared with those made by large-scale materials (such as “bulk”), various potential applications in a wide range of technological fields, which is a crucial factor in the growth of this industry, are generated [1]. TiO_2 is a stable, nonvolatile, and extremely insoluble compound, and it has a refractory quality because of its low thermal conductivity. TiO_2 is amphoteric, although it is more acidic than basic. It is also polymorphic, and it can be found in nature in three different crystallographic forms: anatase tetragonal, brookite orthorhombic, and rutile tetragonal. The brookite phase is unstable and difficult to synthesize. Given these challenges, this mineral sparks minimal interest from a scientific perspective. The anatase and rutile phases, in addition to the brookite phase, can be found in nature, but artificially creating the brookite phase in the laboratory is not difficult. These two varieties of crystal exhibit remarkable distinguishing characteristics. Crystan’s rutile phase has a structure that is denser and more compact than the anatase phase in which it originally existed [2], which has a high refractive index and a higher density and is the more stable form, has these characteristics. TiO_2 is typically regarded as a material that is nontoxic and chemically inert. It has been utilized in various industrial applications, such as white pigments, gas sensors, corrosion-protective and optical layers [3], solar cells [4], environmental purification [5], high dielectric constants and high electrical resistances [6,7], TiO_2 decomposition, and because of its catalytic activities, hydrogen gas generation [8]. In addition to these applications, it can be coated on glass to create a type of glass that cleans itself [9]. Through the sol-gel method, this research showed that TiO_2 can show an anatase phase at temperatures as low as 450 °C and a rutile phase at temperatures as high as 900 °Celsius.

Experimental

1- Synthesis of TiO_2 NP powder via the sol-gel method

The initial materials consisted of $TiCl_4$ with a purity level of 99.99% (BDH, England) and ethanol-CH_3CH_2OH with a purity level of 99.99 %. (GCC,U.K) The synthesis procedure was completed by introducing a series of droplets derived from $TiCl_4$ into an absolute ethanol solution at a ratio of 1:10. The reaction was conducted in the chemical fume hood with the help of a magnetic stirrer to remove toxic gases that were not wanted, such as cloud HCl, while keeping the temperature at room temperature. The formation procedure resulted in the production of a solution that was pale yellow in color and had a pH that fell somewhere in the range of 1.4–2. After subjecting the obtained solution to a temperature of 80 °C for a period of 12 hours, the gel state was successfully achieved. Through calcination, the Anatase phase was obtained at 450 °C in 1.5 hours, by contrast, the Rutile phase was obtained at 900 °C in 1.5 hours.

2- Characterization Techniques

TiO_2 NPs were characterized by an X-ray diffraction device (Lab-X XRD-6000 diffractometer; Shimadzu, Japan). Field emission scanning electron microscopy (FESEM) (MIRA3, TE-SCAN), (IR Affinty-1CE (FTIR) spectrophotometer, Shimadzu, Japanese company) and UV–VIS-NIR spectrophotometer (Shimadzu, UV-1800).

Results and Discussion

1. X-ray Diffraction Analysis

X-ray diffraction analysis was conducted to determine the structure and the phases of TiO_2 NPs. Figure (1) shows almost all the crystal types in the spectrum at 450 °C. The intensity peaks have a polycrystalline nature with a tetragonal structure in the Anatase phase oriented at diffraction angles 2θ at 25.52°, 37.04°, 38.01°, 38.67°, 48.23°, 54.09°, 55.26°, 62.87°, 68.95°, 70.43°, and 75.25° with diffraction planes (101), (103), (004), (112), (200), (105), (211), (204), (116), (220), and (215), respectively. These findings are in line with the card number that was given out by the International Center for Diffraction Data (ICDD), i.e., 21-1272, and they are agrees with the other studies [10,11]. The same figure illustrates the peaks of polycrystalline TiO_2 with a tetragonal structure in the Rutile phase at 900 °C oriented at diffraction angles 2θ of 27.55°, 36.17°, 39.31°, 41.33°, 44.14°, 54.41°, 56.72°, 62.82°, 64.14°, 69.10°, 69.88°, and 76.40° with diffraction planes (110), (101), (200), (111), (210), (211), (220), (002), (310), (301), (112) and (202), respectively. These findings are in line with the card number that was given out by the ICDD, i.e., 21-1276, and they are agrees with the other studies [10]. From pervious results the intensity of the X-ray diffraction increases with growing temperature because of the agglomeration of particles, and the crystalline phase of TiO_2 converted from Anatase phase to Rutile phase. In addition, it can be identified that when the crystallite size increases, the peak of diffraction becomes narrow than the TiO_2 calcite at 900°C. In the present investigation, the crystallite size was determined using Scherrer's formula [11].

$D = 0.9\ \lambda/(\beta \cos\theta)$ ……. (1)

where D represents the size of the crystallite, λ represents the X-ray wavelength of the CuKα line radiation and it is value 1.54056 A, β represents the full width half maximum, and θ represents Bragg's angle. The Anatase and Rutile phases each have their own unique crystallite sizes, which are 15.89 nm and 40.54 nm, respectively.

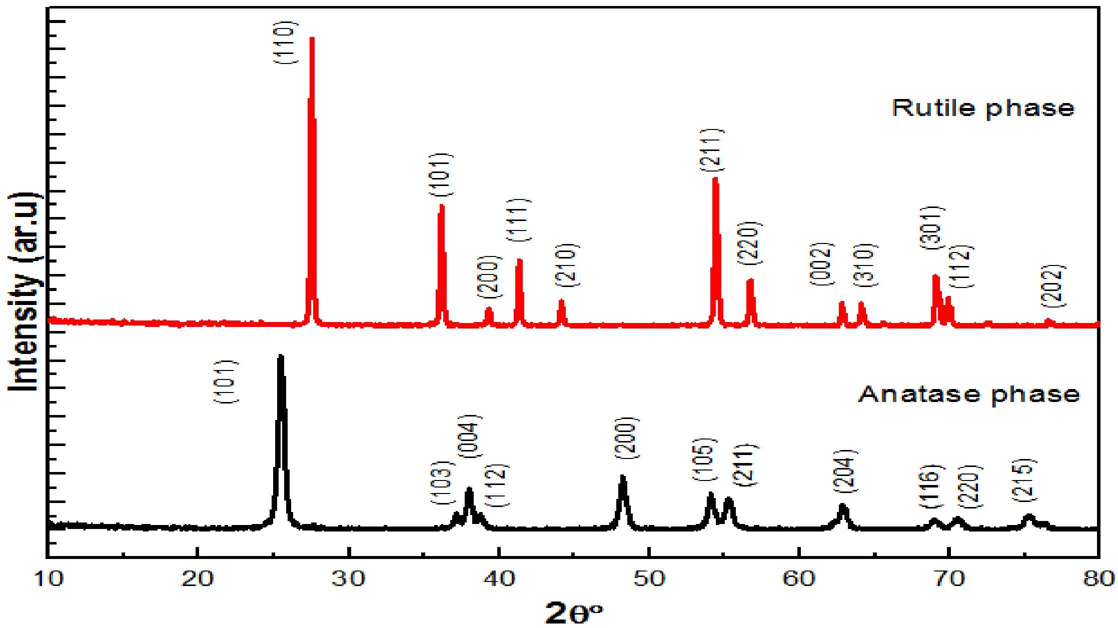

Figure 1: X-ray diffraction patterns of TiO_2 Np.

2. FE-SEM and EDS analysis

A field emission scanning electron microscope (FE-SEM), which scans the surfaces with high magnification and high precision, was used to study the surface topography of the TiO_2 Np. The images of all the prepared materials, magnified at a ratio of 70KX and 135KX, are displayed here. TiO_2 NPs (Anatase phase) have cauliflower-like shapes with small particle sizes, as illustrated in Figure (2a). These results agree with those reported in another study [11]. Rutile phase grains appear in the form of irregular shapes with sizes larger than the Anatase phase size, as shown in Figure (2b). These results agree with those reported by other results

[12]. The Anatase phase has an average particle size of 36.9 nm, whereas the Rutile phase has a size of 58 nm on average. While the temperature is raised to 900 °C, the size of the rutile phase of the TiO_2 NPs increases, causing it to become larger, Accumulation also becomes more remarkable. This result lends credence to the findings of our XRD analysis regarding the size of the particles. The reason for this is that an increase in temperature causes an increase in the kinetic energy of the atoms, which in turn makes it simpler for the atoms to occupy their appropriate positions within the crystal lattice. Consequently, the Grain size increases, resulting in an increase in the overall particle size [13].

a

b

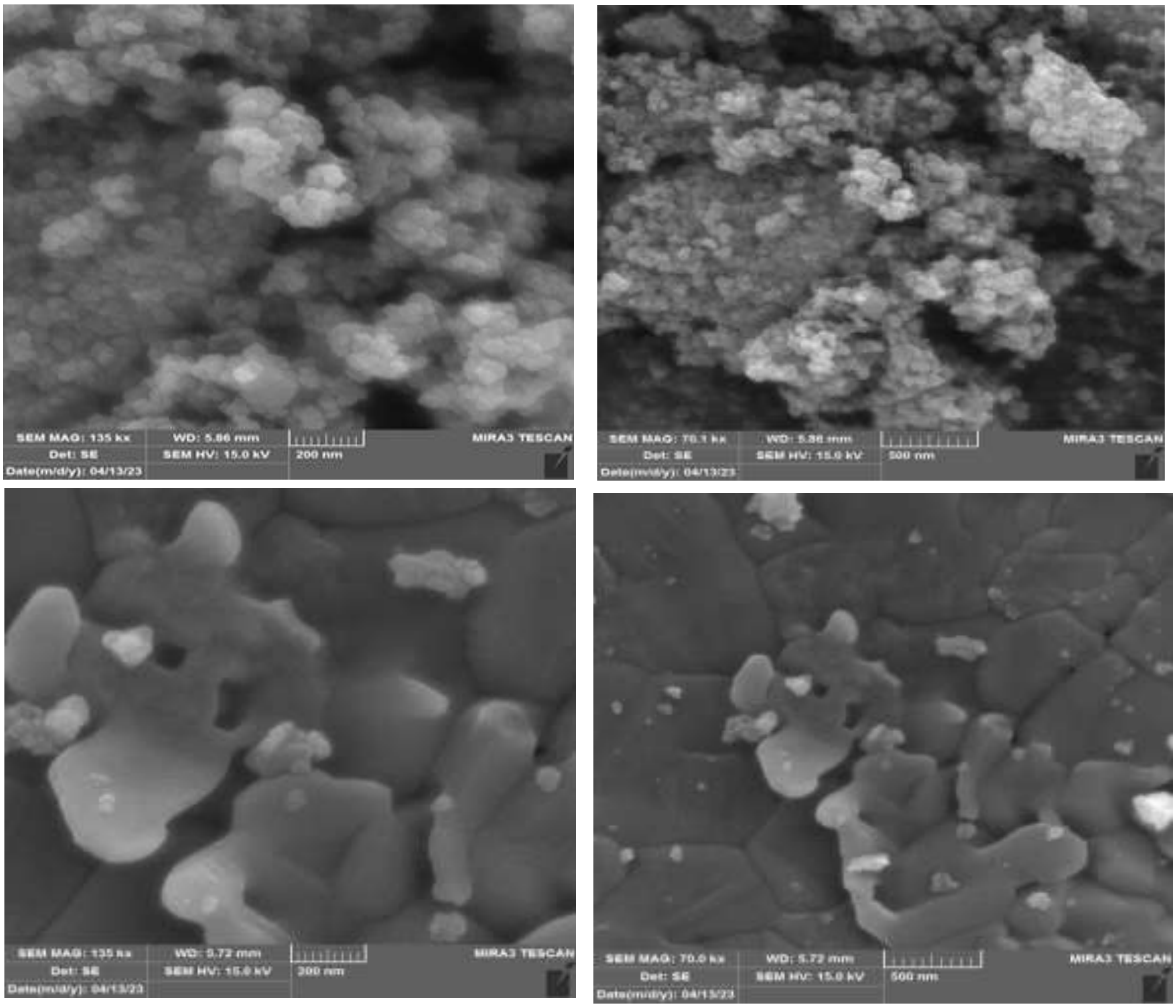

Figure 2: FESEM diffraction patterns of TiO_2 Np (a) Anatase phase (b) Rutile phase.

Academic Science Journal

Through EDS spectra, the elemental composition of the chemical compounds that went into the prepared material was investigated. The EDS spectra of the synthesized TiO_2 NPs are presented in Figure 3. Ti and O are elements that can be found in the anatase and rutile phases of the TiO_2 NPs that were synthesized. This result agrees with the findings of other studies [10]. In TiO_2 NPs, the content of Ti is higher than that of O, and the atomic and weight percentages of TiO2 are tabulated in Figure (3).

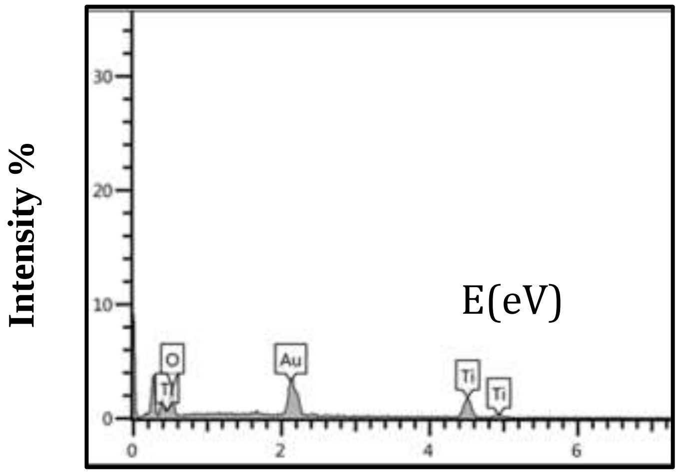

S.no	W (%)
1- Ti	77.5
2- O	22.5

Figure 3: EDS spectra of TiO_2 Np.

3. FTIR analysis

Fourier transform infrared spectroscopic analysis was conducted to understand the interaction between NPs and capping agents. The presence of a broad band at 450–4000 cm^{-1} in the FTIR spectra of TiO_2 NPs corresponds to the stretching vibration of terminating hydroxyl groups in samples. The spectra of TiO_2 (Anatase phase) exhibited prominent peaks at 459, 826, 1324, 1523, 1616, 3240, and 3731 cm^{-1}, as shown in Figure 4. The peaks correspond to Ti–O, Ti–O–Ti, C–H bending, C–H bending C=O stretching, O=H stretching, and O=H stretching, which agrees with the result in [14]. Figure 4 shows that the spectra of TiO_2 (Rutile phase) exhibited prominent peaks at 509, 1143, 1414, 1553, 1640, 3438, and 3743 cm^{-1}. The peaks correspond to Ti–O, Ti–O–Ti, C–H bending, C–H bending C=O stretching, O=H stretching, and O=H stretching, which agrees with the result in [15].

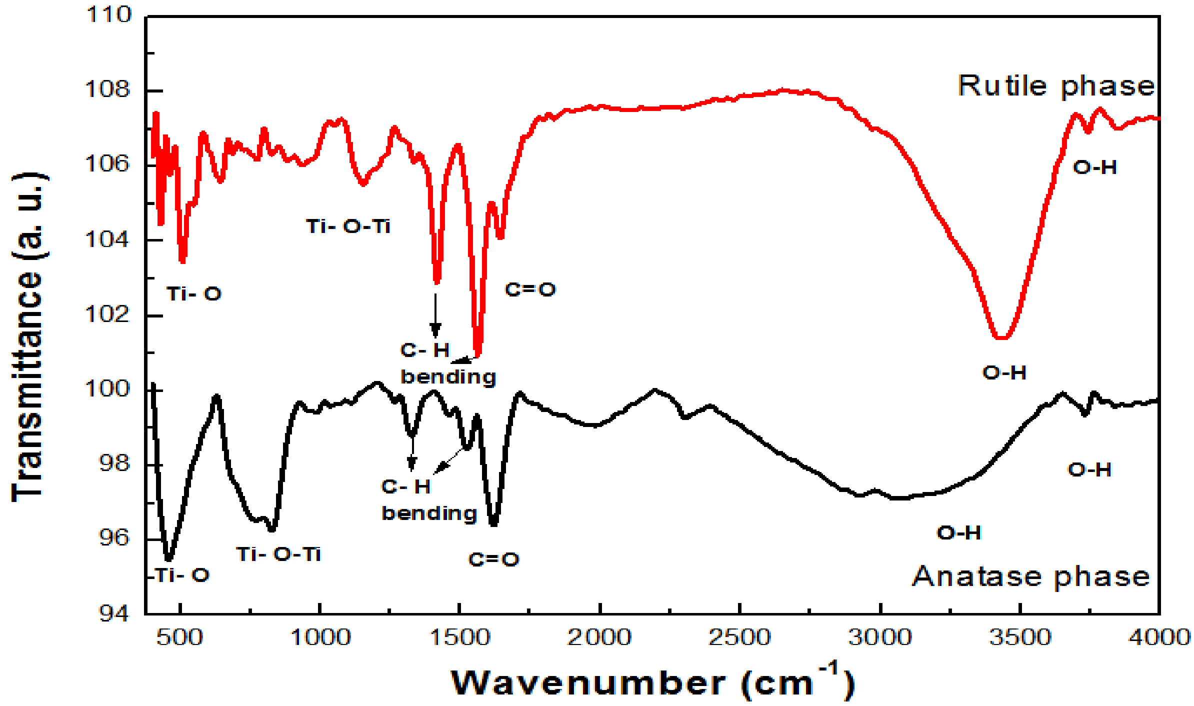

Figure 4: FTIR spectra of TiO_2 Np (Anatase and Rutile) phases.

4. Optical Analysis

UV–Vis-NIR absorbance spectra in the range of 300–900 nm were utilized to study the optical properties of the materials that were prepared. The absorbance spectra of TiO_2 (Anatase and Rutile phases) are depicted as a function of the wavelength in Figure (5). The absorption of TiO_2 increases with an increase in the wavelength range of 300–350 nm. However, once it passes through this region, the absorption begins to decrease gradually with an increase in wavelength. The absorption of TiO_2 in its Anatase phase is lower than that of TiO_2 in its Rutile phase, as shown in the figure, which is consistent with the reported [16]. The values of the optical energy gap (Eg) can be calculated by using Tauc's relation [16], which is as follows:

$$\alpha h\upsilon = B_{\circ}(h\upsilon - E_g^{opt})^r \ldots\ldots (2)$$

where hv represents the energy of the photon, and *B* is a constant which does not depend on photon energy and *r* has four numeric values, (1/2) for allowed direct, 2 for allowed indirect, 3 for forbidden direct and (3/2) for forbidden indirect optical transitions.

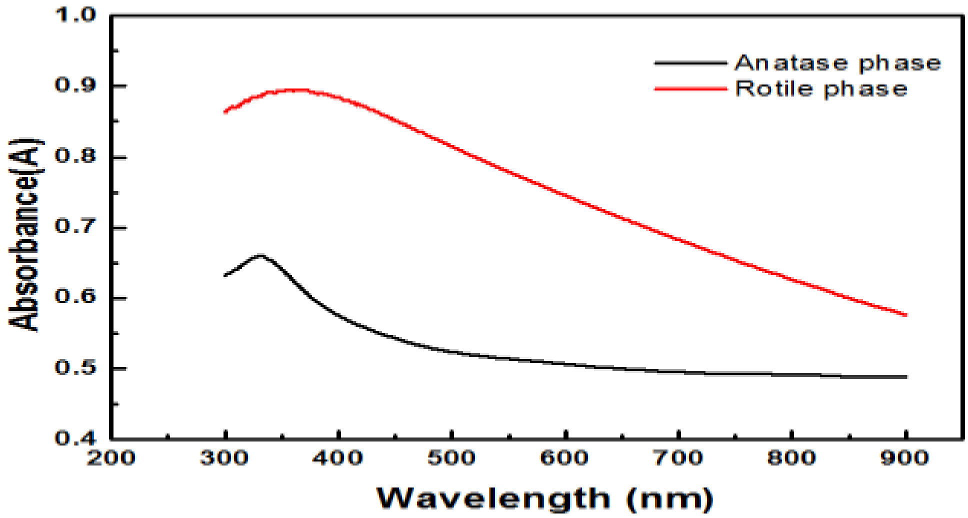

Figure 5: Absorption spectra of TiO2 Np Anatase and Rutile phases.

Figure 6 displays the plot of $(\alpha h\upsilon)^2$ versus h and then calculates the energy gap (Eg) value. From the figure, the energy band gaps are 3.05 eV and 2.7 eV for the Anatase and Rutile phases, respectively, which agrees with the reported values [16]. The reason for the decrease in the optical energy gap with increasing temperature is due to the increase in crystal size, the decrease in grain boundaries, and the reduction in crystal defects [13]. This result is consistent with the XRD and FESEM results (the values of each of the prepared crystal sizes, moreover, grain size rates increase with the increasing temperature of TiO_2 NPs).

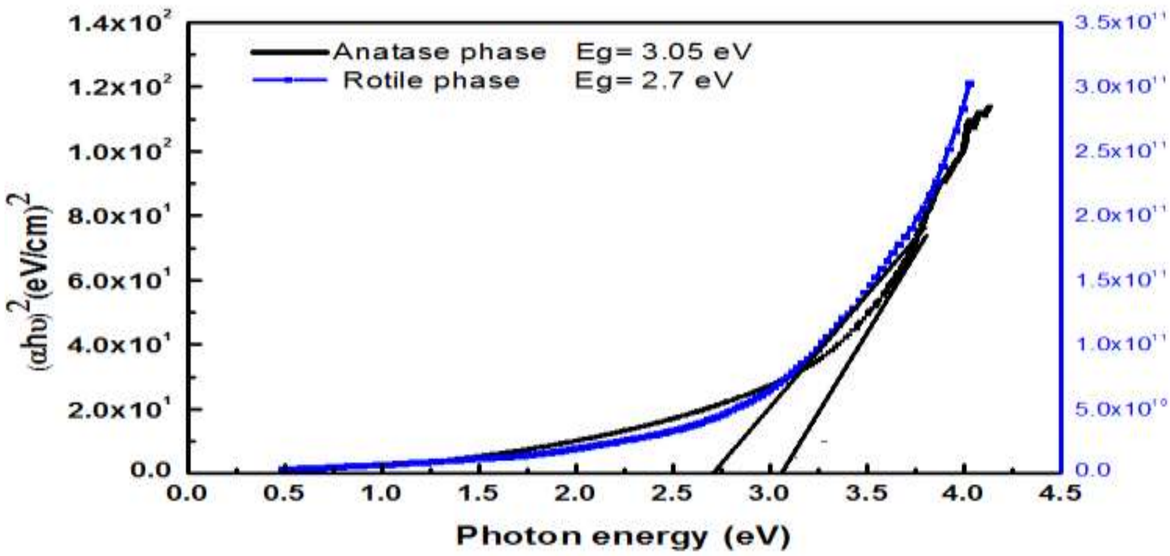

Figure 6: The relation between $(\alpha h\upsilon)^2$ and $(h\upsilon)$ of TiO_2 Np Anatase and Rutile phases.

Conclusions

The TiO_2 Np has been synthesized by the Sol-gel method. The crystallite size of the prepared TiO_2 nanoparticles was approximately 15.89 nm for the Anatase phase and 40.54 nm for the Rutile phase, respectively, confirmed by the XRD graph. The results of the FESEM revealed the formation of nanostructures with cauliflower and irregular shapes, with an average particle size of 36.9 nm for Anatase and 58 nm for Rutile, respectively. The optical measurements show that the absorption of TiO_2 (Anatase phase) is less than that of TiO_2 (Rutile phase), and the optical energy gap is (3.05 eV) and (2.7 eV) for the Anatase and Rutile phases respectively. From these properties, we conclude that the TiO_2 Np can be used as an effective material layer for perovskite solar cells and photocatalytic applications.

References

1. A. P. Alivisatos, A.L. Harris, N.J. Levinos, M.L. Steigerwald, L.E. Brus, Electronic states of semiconductor clusters: homogeneous and inhomogeneous broadening of the optical-spectrum, Journal of Chemical Physics,89, 4001-4011(1998), DOI(https://doi.org/10.1063/1.454833)
2. G. P. Casali, Pigmentos de TiO_2 dopado com os metais de transicao cromo e manganes. Tese de Mestrado, Departamento de Quimica, Univ-ersidade Federal de Sao Carlos, Sao Carlos-SP, (2001)
3. B. R. Sankapal, M.C. Lux-Steiner, A. Ennaoui, Synthesis and characterization of anatase-TiO2 thin films, Applied Surface Science, 239, 165-170(2005), DOI(https://doi.org/10.1016/j.apsusc.2004.05.142)
4. B. O. Regan, M. Gratzel, A low-cost, high-efficiency solar cell based on dyesensitized colloidal TiO2 films, Nature, 353, 737-740(1991), DOI(https://doi.org/10.1038/353737a0)
5. S. Ikezawa, H. Homyara, T. Kubota, R. Suzuki, S. Koh, F. Mutuga, T. Yoshioka, A. Nishiwaki, Y. Ninomiya, M. Takahashi, K. Baba, K. Kida, T. Hara, T. Famakinwa, Applications of TiO_2 film for environmental purification deposited by controlled electron beam-excited plasma, Thin Solid Films, 386, 173-176(2001), DOI(https://doi.org/10.1016/S0040-6090(00)01638-2)

6. H. Cheng, J. Ma, Z. Zhao, L. Qi, Hydrothermal preparation of uniform nanosize rutile and anatase particles, Chemistry of Materials, 7, 663-671(1995), DOI(https://doi.org/10.1021/cm00052a010)
7. M. Gopal, W. J. M Chan, L. C. de Jonghe, Room temperature synthesis of crystalline metal oxides, Journal of Materials Science, 32, 6001-6008(1997), DOI(https://doi.org/10.1023/A:1018671212890)
8. M. A. Fox, M. T. Dulay, Heterogeneous photocatalysis, Chemical Reviews, 93, 341-357(1993), DOI(https://doi.org/10.1021/cr00017a016)
9. E. M. Paula, Silva: A tecnologia, suas estrategias, suas trajetorias. Ciencia e Cultura, 60, 13-21 (2008)
10. A. Saka, Y. Shifera, L. T. Jule, B. Badassa, N Nagaprasad, R Shanmugam, L P. Dwarampudi, V. Seenivasan, K. Ramaswamy, Biosynthesis of TiO_2 nanoparticles by caricaceae (Papaya) shell extracts for antifungal application, Scientific Reports, 12, 1-10(2022), DOI(https://doi.org/10.1038/s41598-022-19440-w)
11. K. S. Landage, G. K Arbade, P. Khanna, C. J Bhongale, Biological approach to synthesize TiO_2 nanoparticles using staphylococcus aureus for antibacterial and anti-biofilm applications, Journal of Microbiology & Experimentation, 8, 36 - 43(2020)
12. Zainab N. Jameel, Olfat A. Mahmood and Faisal L. Ahmed, Studying the Effect of Synthesized Nano-Titanium Dioxide via Two Phases on the Pseudomonas Aeruginosa and Portus Bacteria as Antimicrobial Agents, International Journal of Nanoelectronics and Materials, 12(3), 329-338 (2019),
13. W. Daranfed, M. S. Aido, A. Hafdallah and H. Lekiket, Substrate Temperature Influence on ZnS Thin Films Prepared by Ultrasonic Spray, Thin Solid Films, 518, 1082-1084(2009), DOI(https://doi.org/10.1016/j.tsf.2009.03.227)
14. M. Aravind, M. Amalanathan, M. S. M. Mary, Synthesis of TiO_2 nanoparticles by chemical and green synthesis methods and their multif-aceted properties, SN Applied Sciences, 3, 409- 418 (2021), DOI(https://doi.org/10.1007/s42452-021-04281-5)

15. J. V. M. Zoccal, F. d. O. Arouca, J. A. S Goncalves, Synthesis and characterizationof TiO2 nanoparticles by the method pechini, Materials Science Forum, 2, **385-390**(2010), DOI(https://doi.org/10.4028/www.scientific.net/MSF.660-661.385)

16. S. A. Hamdan, I M Ibrahim, I M Ali, Photodetector based on Rutile and Anatase TiO_2 nanostructures/n-Si heterojunction, Journal of Physics: Conference Series, 2114, 1-9(2021), DOI(10.1088/1742-6596/2114/1/012025)